The method of planes pressure tensor for a spherical subvolume

D. M. Heyes, E. R. Smith, D. Dini, and T. A. Zaki

The method of planes pressure tensor for a spherical subvolume

D. M. Heyes,[a)] E. R. Smith,[b)] D. Dini,[c)] and T. A. Zaki[d)]
Department of Mechanical Engineering, Imperial College London, Exhibition Road, South Kensington, London SW7 2AZ, United Kingdom

Various formulas for the local pressure tensor based on a spherical subvolume of radius, *R*, are considered. An extension of the Method of Planes (MOP) formula of Todd *et al.* [Phys. Rev. E **52**, 1627 (1995)] for a spherical geometry is derived using the recently proposed Control Volume formulation [E. R. Smith, D. M. Heyes, D. Dini, and T. A. Zaki, Phys. Rev. E **85**, 056705 (2012)]. The MOP formula for the purely radial component of the pressure tensor is shown to be mathematically identical to the Radial Irving-Kirkwood formula. Novel offdiagonal elements which are important for momentum conservation emerge naturally from this treatment. The local pressure tensor formulas for a plane are shown to be the large radius limits of those for spherical surfaces. The radial-dependence of the pressure tensor computed by Molecular Dynamics simulation is reported for virtual spheres in a model bulk liquid where the sphere is positioned randomly or whose center is also that of a molecule in the liquid. The probability distributions of angles relating to pairs of atoms which cross the surface of the sphere, and the center of the sphere, are presented as a function of *R*. The variance in the shear stress calculated from the spherical Volume Averaging method is shown to converge slowly to the limiting values with increasing radius, and to be a strong function of the number of molecules in the simulation cell. © *2014 AIP Publishing LLC*. [http://dx.doi.org/10.1063/1.4862915]

I. INTRODUCTION

In various applications, it is useful to be able to resolve the pressure or stress tensor at an atomistic scale based on a subset of the molecules, measured either across a given plane in space or with respect to a small volume containing just a few molecules. The literature on such "local" stress definitions is extensive and largely based on the formula for the stress tensor at a point derived in the pioneering paper by Irving and Kirkwood (IK).[1] The original IK formula cannot be calculated in practice in molecular simulation, but has formal significance, and relaxed approximations or integrated extensions of it can be computed. It is the integrated extensions of the IK formula which will be considered here. There are now three main formulas in widespread use. The first is an integration of Irving and Kirkwood's original formula at a point to cover a flat plane,[2] or curved (spherical) surfaces,[3–9] which we call the Planar Irving Kirkwood (PIK) method and Radial Irving Kirkwood (RIK) methods, respectively. The second method takes a weighted average of the contributions from molecules which are located inside or have pair interactions which cross within an arbitrarily shaped volume, which we call the Volume Averaging (VA) formula,[10–12] again this can be derived directly from Irving and Kirkwood's point pressure tensor formula. The third formula is the Method of Planes (MOP) of Todd *et al.*,[13] which gives the tractions acting at a flat plane, and therefore those elements of the pressure tensor containing the direction perpendicular to the plane as one of the Cartesian directions. The MOP pressure is widely used

in the literature,[14–18] can be applied in arbitrary geometries, avoids spurious oscillations,[13] is consistent with the simple definition of stress over a plane[19] and can be shown to be exactly equal to change in momentum of an associated control volume.[20] As simple liquids, glasses and many amorphous materials are isotropic, a sphere is the natural shape to base a definition of a local stress. The extension of the local pressure tensor methodology to a spherical boundary or subvolume is the subject of this work.

In Sec. II, various formulas for calculating the local pressure tensor are presented and compared. The focus is on the extension of the flat plane formulas to a (virtual) spherical boundary of a spherical subvolume in a bulk liquid. Physical surfaces are not considered here and therefore surface tension effects do not enter the description. The measurements are taken over a purely conceptual surface in line with the fundamental definition of stress. The geometry considered here is an open subvolume within a large system. The discussion of the local pressure tensor formulas is framed in the context of molecular simulation, although their use is more general. In Sec. III, the properties and underlying statistics of these formulas are investigated using Molecular Dynamics simulations.

II. THEORY

In the bulk liquid state the pressure tensor, $\underline{\underline{P}}$, is usually calculated in molecular simulation by the virial formula,[21]

$$\underline{\underline{P}} = \frac{1}{V_{sim}} \left\langle \sum_{i=1}^{N} \frac{1}{m_i} \underline{p}_i \underline{p}_i - \frac{1}{2} \sum_{i=1}^{N} \sum_{j \neq i}^{N} \frac{\underline{r}_{ij} \underline{r}_{ij}}{r_{ij}} \phi'_{ij}(r_{ij}) \right\rangle, \quad (1)$$

a)Electronic mail: d.heyes@imperial.ac.uk
b)Electronic mail: edward.smith05@imperial.ac.uk
c)Electronic mail: d.dini@imperial.ac.uk
d)Electronic mail: t.zaki@imperial.ac.uk

where V_{sim} is the volume of the simulation cell (usually of cubic shape) containing N molecules, i is the index of the molecule, and m_i is its mass. The angular brackets denote an ensemble or time average. The pressure tensor is composed of kinetic (k) and configurational (c) components, which are the first and second terms on the right of the expression in Eq. (1), respectively. If $\underline{r}_i$ is the co-ordinate of particle, i, then $\underline{r}_{ij} = \underline{r}_i - \underline{r}_j$. The bulk pressure for an isotropic equilibrium fluid is $P = (P_{xx} + P_{yy} + P_{zz})/3$. The translational peculiar momentum is $\underline{p}_i$,

$$\underline{p}_i = m_i(\underline{v}_i - \underline{u}(\underline{r} = \underline{r}_i)), \qquad (2)$$

where $\underline{v}_i$ is the laboratory frame velocity of molecule i and $\underline{u}$ is the local advected or "streaming" velocity at spatial position $\underline{r}$. For notational simplicity, it will be assumed that the system is composed of monatomic molecules and that the pair potential, ϕ_{ij}, is radially symmetric. In the above equation, the standard notation, $\phi'_{ij} \equiv d\phi_{ij}/dr_{ij}$, is used.

Following Irving and Kirkwood,[1] the pressure tensor at point $\underline{r}$ is

$$\underline{\underline{P}}(\underline{r}) = \underline{\underline{P}}^k(\underline{r}) + \underline{\underline{P}}^c(\underline{r}), \qquad (3)$$

where

$$\underline{\underline{P}}^k(\underline{r}) = \left\langle \sum_{i=1}^N \frac{\underline{p}_i \underline{p}_i}{m_i} \delta(\underline{r} - \underline{r}_i) \right\rangle, \qquad (4)$$

and δ is the Dirac delta function. For an isotropic fluid at equilibrium, $\underline{\underline{P}}^k(\underline{r}) = k_B T \rho(\underline{r}) \underline{\underline{I}}$, where k_B is Boltzmann's constant, T is the temperature, $\rho(\underline{r})$ is the number density at $\underline{r}$, and $\underline{\underline{I}}$ is the unit tensor. The configurational part of the pressure tensor at $\underline{r}$ is[5,22]

$$\underline{\underline{P}}^c(\underline{r}) = -\frac{1}{2} \left\langle \sum_{i=1}^N \sum_{j \neq i} \frac{\partial \phi_{ij}}{\partial \underline{r}_{ij}} \int_{Cij} d\underline{l} \delta(\underline{r} - \underline{l}) \right\rangle, \qquad (5)$$

where Cij is the path from the center of i to j. Being perhaps the most physically reasonable choice, Irving and Kirkwood,[1] chose for Cij a straight line between i and j, i.e., $\underline{l} = \underline{r}_i + \alpha \underline{r}_{ji}$, where $0 \leq \alpha \leq 1$ and $\underline{r}_{ji} = \underline{r}_j - \underline{r}_i$.[1] Equation (5) then reduces to

$$\underline{\underline{P}}^c(\underline{r}) = -\frac{1}{2} \left\langle \sum_{i=1}^N \sum_{j \neq i} \frac{\partial \phi_{ij}}{\partial \underline{r}_{ij}} \underline{r}_{ij} \int_0^1 d\alpha \, \delta(\underline{r} - \underline{r}_i - \alpha \underline{r}_{ji}) \right\rangle \quad (6)$$

using the straight line contour definition. The pressure tensor expressions in Eqs. (4) and (6) are formally related to the time evolution of momentum through,[1]

$$\underbrace{\frac{\partial}{\partial t} \left\langle \sum_{i=1}^N m_i \underline{v}_i \delta(\underline{r} - \underline{r}_i) \right\rangle}_{\text{Accumulation}} + \underbrace{\underline{\nabla} \cdot [\rho(\underline{r}) \underline{u}(\underline{r}) \underline{u}(\underline{r}) + \underline{\underline{P}}^k(\underline{r})]}_{\text{Advection}}$$

$$+ \underbrace{\underline{\nabla} \cdot \underline{\underline{P}}^c(\underline{r}) = 0.}_{\text{Forcing}} \qquad (7)$$

In order to apply the Irving and Kirkwood[1] equations in molecular simulations, the Dirac delta function expression must be transformed to a function which extends over a region in space. In the process of this arbitrary extension, the

exact equality of Eq. (7) is often lost. The pressure definition is known to be non-unique,[22] for various reasons, including choice of interaction contour between molecules (e.g., linear or nonlinear between two molecules, three body interactions and higher), choice of gauge for the pressure tensor and choice of averaging volume and weighting function.[23] Only the point-wise Irving and Kirkwood relations are formally equivalent to the point-wise continuum equations (i.e., the equations defined for a volume of infinitesimal size). The introduction of any finite averaging volume introduces a systematic error, as the pressure is never truly constant inside a finite volume. In continuum fluid mechanics, this problem can be circumvented by expressing the continuum system in the exactly conservative control volume form,[24] and accepting that only surfaces fluxes and changes in a volume can be related exactly. When a molecular system is expressed in terms of control volume, it becomes apparent that only the surface flux forms of pressure (e.g., RMOP) exactly govern the momentum change in the volume these surfaces enclose.

A number of widely used expressions for the local pressure tensor derived from the IK equations (4) and (6) are described in Subsections II A–II F. Where the derivations of the formulas are already in the literature, only the final results are presented. The relationship between the various forms of pressure is then explored using the notion of the control volume. The notation follows a unified format across the different formulas.

A. Planar Irving-Kirkwood

Consider an infinite flat plane geometry with the surface normal in the z direction, and a cross-sectional area of interest, $A = L_x L_y$, where L_x and L_y are the lengths of the simulation domain in the x and y directions. Then the interaction part of the stress is of the form given by, for example, Rao and Berne (1979)[2]

$$\underline{\underline{P}}^c_{IK}(z)$$

$$= -\frac{1}{2A} \left\langle \sum_{i=1}^N \sum_{j \neq i} \frac{\underline{r}_{ij} \underline{r}_{ij}}{r_{ij}} \phi'_{ij} \frac{1}{|z_{ij}|} H\left(\frac{z_i - z}{z_{ij}}\right) H\left(\frac{z - z_j}{z_{ij}}\right) \right\rangle$$

$$= -\frac{1}{2A} \left\langle \sum_{i=1}^N \sum_{j \neq i} \frac{\underline{r}_{ij} \underline{r}_{ij}}{r_{ij}} \phi'_{ij} \frac{1}{|z_{ij}|} H(\alpha_1) H(1 - \alpha_1) \right\rangle, \qquad (8)$$

where $H(x)$ is the Heaviside step function of x, and $\alpha_1 = (z_i - z)/z_{ij}$. The subscript, 1, indicates that the line between i and j can only cross the plane at z a maximum of once. Equation (8), referred to here as the "Planar Irving Kirkwood" (PIK) method, is obtained by integrating the formula in Eq. (6) over the planar area A. The Heaviside functions in Eq. (8) ensure that only those ij pairs whose separation vector crosses the plane are incorporated in the summation. It is usual in equilibrium systems to consider only the so-called normal (N) and tangential (T) components of the pressure tensor, P_N and P_T, respectively, which are related to the total pressure tensor through

$$\underline{\underline{P}}(R) = P_T(\hat{\underline{e}}_x \hat{\underline{e}}_x + \hat{\underline{e}}_y \hat{\underline{e}}_y) + P_N \hat{\underline{e}}_z \hat{\underline{e}}_z, \qquad (9)$$

where $\hat{e}_m$ is the unit vector in the *m*-th cartesian direction. From Eq. (8),

$$P_{IK,N}^c(z) = -\frac{1}{2A}\left\langle \sum_{i=1}\sum_{j\neq i} \frac{z_{ij}}{r_{ij}} \text{sgn}(z_{ij})\phi'_{ij}H(\alpha_1)H(1-\alpha_1)\right\rangle,$$
(10)

where $\phi'_{ij} \equiv d\phi_{ij}/dr_{ij}$, and

$$P_{IK,T}^c(z) = -\frac{1}{4A}\left\langle \sum_{i=1}\sum_{j\neq i} \frac{(x_{ij}^2+y_{ij}^2)}{r_{ij}} \frac{1}{|z_{ij}|}\phi'_{ij}H(\alpha_1)H(1-\alpha_1)\right\rangle.$$
(11)

The kinetic part of the PIK pressure tensor for an equilibrium isotropic liquid is $\rho(z)k_BT$, where $\rho(z)$ is the fluid density at z.

B. Radial Irving-Kirkwood

The pressure tensor for an equilibrium isotropic liquid across a *spherical* surface can be conveniently expressed in polar coordinates,[5] in terms of tangential (*T*) and normal (*N*) components

$$\underline{\underline{P}}(R) = P_T(\hat{e}_{t_1}\hat{e}_{t_1} + \hat{e}_{t_2}\hat{e}_{t_2}) + P_N\hat{e}_n\hat{e}_n,$$
(12)

where R is the radius of the sphere, and $\underline{e}_{t_1}$ and $\underline{e}_{t_2}$ are two orthogonal unit vectors tangential to the surface plane. The unit vector, $\hat{e}_n$, is normal to the surface. The normal component of the pressure tensor in this coordinate system, $P_{IK,N}$ is[4,5]

$$P_{IK,N}(R) = \rho(R)k_BT - \frac{1}{2A}\left\langle \sum_{i=1}\sum_{j\neq i}\sum_{k=1}^{2} \frac{\underline{r}_{ij}.\hat{e}_{n,k}}{r_{ij}}\right.$$
$$\left. \times \text{sgn}(\underline{r}_{ij}.\hat{e}_{n,k})\phi'_{ij}H(\alpha_k)H(1-\alpha_k)\right\rangle,$$
(13)

where $\rho(R)$ is the number density at radius R from the center of the sphere, $A = 4\pi R^2$, α_k is one of the two roots given by the intersection of the sphere with the line between molecules i and j. The quantity $\hat{e}_{n,k} \equiv \underline{R}_k/R_k$ is the unit vector from the center of the sphere to where $\underline{r}_{ij}$ crosses the surface of the sphere for the k-th time. Equation (13) is referred to as the RIK expression here. The origins of the vectors $\underline{r}_i$ and $\underline{r}_j$ are for this analysis taken to be at the center of the sphere. The $\underline{r}_{ij}$ vector can cross the sphere's surface a maximum of two times which is taken account of in the above formula through the k index (recall the single root is denoted by α_1 in the corresponding planar-geometry formula in Eq. (8)). Central to the application of this equation is a method for obtaining the points of intersection, α_k, discussed below and in Appendix A. By analogy with Eq. (11), taking a local plane orthogonal to the vector between the intersection of $\underline{r}_{ij}$ with the sphere and the origin of the sphere, for the tangential component,

$$P_{IK,T}(R) = \rho(R)k_BT - \frac{1}{4A}\left\langle \sum_{i=1}\sum_{j\neq i}\sum_{k=1}^{2}((\underline{r}_{ij}.\hat{e}_{t_1,k})^2\right.$$
$$\left. + (\underline{r}_{ij}.\hat{e}_{t_2,k})^2)\frac{1}{r_{ij}|\underline{r}_{ij}.\hat{e}_{n,k}|}\phi'_{ij}H(\alpha_k)H(1-\alpha_k)\right\rangle,$$
(14)

for an equilibrium isotropic liquid. The RIK equations (13) and (14) go over to the PIK formulas (10) and (11), respectively, as the radius, R, tends to infinity compared to the molecular diameter.

C. Control volume

In this subsection, a selecting function is derived in terms of the Heaviside function. This is used to obtain the VA pressure tensor and then applied to demonstrate the link between the VA pressure tensor and the Method of Planes pressure tensor. This has the clear advantage of providing a formal equality between the method of planes pressure tensor for a spherical geometry and the time evolution inside the selecting function, as in the Irving and Kirkwood[1] equations (7). Integration of the Dirac delta function in Eqs. (4) and (6) $\delta(\underline{r} - \underline{r}_\kappa)$, over a volume in space defines a "selection function," ϑ, for that volume and shape.[20] This function is non-zero only if r_κ is inside the volume of interest and is defined as

$$\vartheta_\kappa \equiv \int_V \delta(\underline{r} - \underline{r}_\kappa)dV.$$
(15)

The vector $\underline{r}_\kappa$ can be the location of molecule i as in Eq. (4), in which case the following quantity:

$$\vartheta_i \equiv \int_V \delta(\underline{r} - \underline{r}_i)dV,$$
(16)

is defined. Of special interest here, $\underline{r}_\kappa$ can represent any point on the straight line $\underline{r}_{ij}$ between molecules i and j as in Eq. (6), in which case, $\underline{r}_\kappa = \underline{r}_i + \alpha\underline{r}_{ji}$, where $\underline{r}_{ji} = \underline{r}_j - \underline{r}_i$. This continuous variable must be in the range, $0 \leq \alpha \leq 1$ for the particle to be in the volume. The fraction of r_{ij} which crosses the volume, ℓ_{ij} has the formal definition,

$$\ell_{ij} \equiv \int_0^1 \vartheta_\kappa(\alpha)d\alpha \equiv \int_0^1\int_V \delta(\underline{r} - \underline{r}_i - \alpha\underline{r}_{ji})dVd\alpha.$$
(17)

The selection function is therefore a construction of general utility which can be used to establish if a molecule is in a subvolume or CV, from Eq. (16), or what fraction of the line between the two molecules is in that subvolume, from Eq. (17).

For a spherical CV, it is convenient to locate the origin of the coordinate system at the center of the sphere, $\underline{r}_o$. The Delta function is expressed in polar coordinates,[5]

$$\delta(\underline{r} - \tilde{\underline{r}}_\kappa) = \frac{1}{|\underline{r}|^2\sin\theta}\delta(|\underline{r}| - |\tilde{\underline{r}}_\kappa|)\delta(\theta - \theta_\kappa)\delta(\phi - \phi_\kappa),$$
(18)

where $\tilde{r}_\kappa = r_\kappa - r_o$, the three polar coordinates are r_κ, θ_s and ϕ_s, and where the arguments of the delta functions are scalars. For subsequent notational simplicity $|\tilde{r}_\kappa|$ is written as r_κ. The integral over a spherical shell volume element, $dV = r^2 \sin\theta \, d\phi \, d\theta \, dr$ is

$$\vartheta_\kappa = \int_V \delta\left(r - \tilde{r}_\kappa\right) dV = \int_0^R dr \int_0^\pi d\theta \int_0^{2\pi} d\phi \, \delta\left(r - r_\kappa\right)$$
$$\times \delta\left(\theta - \theta_\kappa\right)\delta\left(\phi - \phi_\kappa\right)$$
$$= [H\left(R - r_\kappa\right) - H\left(-r_\kappa\right)][H\left(\pi - \theta_\kappa\right) - H\left(-\theta_\kappa\right)]$$
$$\times [H\left(2\pi - \phi_\kappa\right) - H\left(-\phi_\kappa\right)]. \qquad (19)$$

The radius must be positive so, $H(-r_\kappa) = 0$ for all r_κ. The Heaviside functions involving the angles confine them to the ranges, $0 < \theta < \pi$ and $0 < \phi < 2\pi$. The expression for the spherical CV function in Eq. (15) can therefore be simplified to

$$\vartheta_\kappa = H\left(R - r_\kappa\right). \qquad (20)$$

Using this result, the IK momentum conservation Eq. (7) can be expressed in the control volume form[20] (rather than a point in space) as

$$\underbrace{\frac{\partial}{\partial t}\left\langle \sum_{i=1}^N m_i \underline{v}_i \vartheta_i \right\rangle}_{\text{Accumulation}} = -\int_V \underline{\nabla} \cdot \underbrace{[\rho \underline{u}\underline{u} + \underline{\underline{P}}^K(\underline{r})}_{\text{Advection}} + \underbrace{\underline{\underline{P}}^C(\underline{r})]}_{\text{Forcing}} dV,$$
$$\qquad (21)$$

where ϑ_i is included on the left hand side of the above equation, which is equal to 1 if the center of the molecule is in volume V and zero otherwise. The average pressure tensor for these pointwise pressure tensors, Eqs. (4) and (6) integrated over a spherical volume, is presented in Sec. II D. In Sec. II E, the link between these spherical VA pressure tensor and the MOP formulas across the surface is derived. It is then demonstrated that Eq. (21) only holds exactly for the MOP form.

D. Volume averaging

Spatial integration of the pointwise IK formula in Eqs. (4) and (6) can be used to obtain the average value of the pressure tensor in a subvolume V of arbitrary shape.[10–12,25] This leads to the so-called "Volume Averaging" or VA method.[26] The VA definition of the pressure tensor ascribes an average value for the whole subvolume through the approximation,

$$\int_V \underline{\underline{P}}(\underline{r}) dV = \int_V [\underline{\underline{P}}^K(\underline{r}) + \underline{\underline{P}}^C(\underline{r})] dV \approx V \underline{\underline{P}}^K_{VA} + V \underline{\underline{P}}^C_{VA}. \qquad (22)$$

The kinetic term is

$$\underline{\underline{P}}^k_{VA}(V) = \frac{1}{V}\left\langle \sum_{i=1}^N \frac{1}{m_i} \underline{p}_i \underline{p}_i \vartheta_i \right\rangle, \qquad (23)$$

with ϑ_i being the CV function of Eq. (20), where $\underline{r}_\kappa = \underline{r}_i$. The configurational term is

$$\underline{\underline{P}}^c_{VA}(V) = -\frac{1}{2V}\left\langle \sum_{i=1}^N \sum_{j \neq i}^N \frac{\underline{r}_{ij}\underline{r}_{ij}}{r_{ij}} \phi'_{ij}(r_{ij}) \ell_{ij} \right\rangle. \qquad (24)$$

The dimensionless parameter, ℓ_{ij}, is the fraction of r_{ij} inside V, given by substituting Eq. (20) in Eq. (17). An approximate solution for ℓ_{ij} can be obtained by sub-dividing the interaction line into a number of segments and assigning these "stresslets" to the appropriate volume.[27] However, for an exact solution, the equation inside the Heaviside function $\vartheta_\kappa(\alpha)$ must be solved analytically. Here, $\underline{r}_\kappa = \underline{r}_i - \alpha \underline{r}_{ij}$ is a quadratic with two roots, which is not trivial to integrate directly with respect to α. Instead the roots of the equation can be used to provide the exact length of interaction inside the volume (see Appendix A). A thin spherical shell of average radius R could also be used for V, which in the limit of $R \to \infty$ will go over to the formulas discussed in Ref. 26, for an infinitely thin planar volume, in which case the VA formula give the same result as the RIK formulas, (13) and (14), as shown in Appendix B.

E. Method of planes

The MOP formula[13] is consistent with the mechanical definition of stress as it uses the pair forces which cross a flat plane.[19] It is derived for a plane located at z by assuming a uniform fluid in the x and y directions and taking the Fourier transform of the Irving and Kirkwood formula in Eq. (3).[13] The MOP formula for the βz component of the pressure tensor at the plane located at z is

$$P^{\beta z}_{MOP}(z) = \frac{1}{A}\left\langle \sum_{i=1}^N \frac{1}{m_i} p_{\beta i} p_{zi} \delta(z - z_i) \right\rangle - \frac{1}{4A}$$
$$\times \left\langle \sum_{i=1}^N \sum_{j \neq i}^N \frac{r_{\beta ij}}{r_{ij}} \phi'_{ij}(r_{ij}) \text{sgn}(z_{ij}) H(\alpha_1) H(1 - \alpha_1) \right\rangle,$$
$$\qquad (25)$$

for the kinetic and configurational parts, respectively. The β component of $\underline{r}_{ij}$ is denoted by $r_{\beta ij}$. The quantity, α_1 is the value of α in Eq. (6) where the vector $\underline{r}_{ij}$ crosses the plane at z. It is the purpose of this section to extend Eq. (25) to the case of a spherical surface. The MOP formulation for a cylindrical surface has been derived in the literature using a Hankel transform.[28] It may be possible to derive the MOP for a spherical surface using a similar approach, however it is more convenient to obtain this using a discrete analogue of Gauss' theorem[20] applied to the right hand side of Eq. (21), as follows:

$$\int_V \underline{\nabla} \cdot (\underline{\underline{P}}^K(\underline{r}) + \underline{\underline{P}}^C(\underline{r})) dV = \oint_S (\underline{\underline{P}}^K(\underline{r}) + \underline{\underline{P}}^C(\underline{r})) \cdot d\underline{S}, \qquad (26)$$

where

$$\int_V \nabla \cdot (\underline{\underline{P}}^K(\underline{r}) + \underline{\underline{P}}^C(\underline{r})) dV$$

$$= \int_V \nabla \cdot \left[\left\langle \sum_{i=1}^{N} \frac{1}{m_i} \underline{p}_i \underline{p}_i \vartheta_i \right\rangle \right.$$

$$\left. - \frac{1}{2} \left\langle \sum_{i=1}^{N} \sum_{j \neq i}^{N} \frac{\underline{r}_{ij}\underline{r}_{ij}}{r_{ij}} \phi'_{ij}(r_{ij}) \int_0^1 \vartheta_\kappa(\alpha) d\alpha \right\rangle \right] dV, \quad (27)$$

from Eqs. (6) and (15). Only the control volume functions, ϑ_i and $\vartheta_\kappa(\alpha)$ are a function of macroscopic position $\underline{r}$. The gradient in radial coordinates of the CV function ϑ_κ is

$$\nabla \vartheta_\kappa = \frac{\partial \vartheta_\kappa}{\partial r} \hat{\underline{e}}_n + \frac{1}{r} \frac{\partial \vartheta_\kappa}{\partial \theta} \hat{\underline{e}}_\theta + \frac{1}{r \sin\theta} \frac{\partial \vartheta_\kappa}{\partial \phi} \hat{\underline{e}}_\phi. \quad (28)$$

As ϑ_κ is not a function of θ or ϕ, the gradient in Eq. (28) can be reduced to

$$\nabla \vartheta_\kappa = \hat{\underline{e}}_n \delta(R - r_\kappa). \quad (29)$$

The kinetic term in Eq. (27) is

$$\int_V \nabla \cdot \left\langle \sum_{i=1}^{N} \frac{1}{m_i} \underline{p}_i \underline{p}_i \vartheta_i \right\rangle dV = \left\langle \sum_{i=1}^{N} \frac{1}{m_i} \underline{p}_i \underline{p}_i \cdot \hat{\underline{e}}_n \delta(R - r_i) \right\rangle$$

$$= \oint_S \underline{\underline{P}}^K(\underline{r}) \cdot d\underline{S}, \quad (30)$$

where $r_\kappa = r_i$ in Eq. (29). The second equality in the above equation follows from the property of the Dirac delta which selects those molecules crossing the surface.[20] Taking the surface average, $\oint_S \underline{\underline{P}}^K(\underline{r}) \cdot d\underline{S} \equiv A\underline{\underline{P}}^k_{MOP}(R)$, the kinetic part of the pressure tensor is

$$\underline{\underline{P}}^k_{MOP}(R) = \frac{1}{A} \left\langle \sum_{i=1}^{N} \frac{1}{m_i} \underline{p}_i \underline{p}_i \cdot \hat{\underline{e}}_n \delta(R - r_i) \right\rangle. \quad (31)$$

Equation (31) can be re-expressed as a summation in terms of particle crossings over time as a generalization of the planar kinetic formula given in Eq. (22) of Ref. 13. This is

$$\underline{\underline{P}}^k_{MOP}(R) = \frac{1}{2A\tau} \sum_{m} \sum_{i=1}^{N} \underline{p}_i(t_{mi}) \text{sgn}[\underline{p}_i(t_{mi}).\hat{\underline{e}}_n], \quad (32)$$

where $\hat{\underline{e}}_n$ is the unit vector from the center of the sphere to the point where molecule, i, crosses the sphere's surface for the m-th time, at time t_{mi}, and where the total elapsed time is τ.

In order to obtain the configurational part of Eq. (27), the following must be evaluated:

$$\int_0^1 \nabla \vartheta_\kappa(\alpha) d\alpha = \hat{\underline{e}}_n \int_0^1 \delta(R - r_\kappa) d\alpha$$

$$= \hat{\underline{e}}_n \int_0^1 \delta(|\underline{R}| - |\underline{r}_i + \alpha \underline{r}_{ji}|) d\alpha. \quad (33)$$

Equation (33) can be expressed in readily computable form using the following relationships for the solution of the Dirac delta of a function with N_r roots,

$$\int_0^1 \delta(g(\alpha)) d\alpha = \sum_{k=1}^{N_r} \int_0^1 \frac{\delta(\alpha - \alpha_k)}{|g'(\alpha_k)|} d\alpha$$

$$= \sum_{k=1}^{N_r} \frac{H(1 - \alpha_k)}{|g'(\alpha_k)|} - \frac{H(0 - \alpha_k)}{|g'(\alpha_k)|}, \quad (34)$$

where $g(\alpha) = |\underline{R}| - |\underline{r}_i + \alpha \underline{r}_{ji}| = 0$. The two roots of quadratic $g(\alpha)$,

$$(\underline{r}_i + \alpha \underline{r}_{ji}) \cdot (\underline{r}_i + \alpha \underline{r}_{ji}) - |\underline{R}|^2 = 0, \quad (35)$$

are given by

$$\alpha_k = \frac{-\underline{r}_{ji} \cdot \underline{r}_i \pm \sqrt{|\underline{r}_{ji} \cdot \underline{r}_i|^2 - |\underline{r}_{ji}|^2 |\underline{R}|^2}}{|\underline{r}_{ji}|^2}. \quad (36)$$

Both roots must be real and at least one must lie in the range $0 \leq \alpha_k \leq 1$ in order to a surface crossing of r_{ji}. The derivative of $g(\alpha)$ is

$$g'(\alpha) = \frac{\partial}{\partial \alpha}(|\underline{R}| - |\underline{r}_i + \alpha \underline{r}_{ji}|) = \frac{\underline{r}_{ji} \cdot [\underline{r}_i + \alpha \underline{r}_{ji}]}{|\underline{r}_i + \alpha \underline{r}_{ji}|}$$

$$= -\underline{r}_{ji} \cdot \hat{\underline{e}}_{n,k}, \quad (37)$$

where $\underline{R}_k = \underline{r}_i + \alpha_k \underline{r}_{ji}$ and $\hat{\underline{e}}_{n,k} = \underline{R}_k/|\underline{R}_k|$. Inserting the formula for $g'(\alpha)$ from Eqs. (37) in (34) gives

$$\int_0^1 \delta(g(\alpha)) d\alpha = \sum_{k=1}^{2} \frac{H(1 - \alpha_k)}{|g'(\alpha_k)|} - \frac{H(0 - \alpha_k)}{|g'(\alpha_k)|}$$

$$= \sum_{k=1}^{2} \frac{1}{|\underline{r}_{ji} \cdot \hat{\underline{e}}_{n,k}|} [H(1 - \alpha_k) - H(-\alpha_k)]. \quad (38)$$

Equation (33) can therefore be re-written as,

$$\int_0^1 \nabla \vartheta_\kappa(\alpha) d\alpha = \sum_{k=1}^{2} \frac{\hat{\underline{e}}_{n,k}}{|\underline{r}_{ji} \cdot \hat{\underline{e}}_{n,k}|} [H(1 - \alpha_k) - H(-\alpha_k)]$$

$$= \sum_{k=1}^{2} \frac{\hat{\underline{e}}_{n,k}}{|\underline{r}_{ji} \cdot \hat{\underline{e}}_{n,k}|} H(\alpha_k) H(1 - \alpha_k),$$

where the sum of $k = 1$ or 2 includes the two possible intersections of the line between i and j with the sphere. The second equality can be verified by comparing the different possible forms obtained by integrating the Dirac delta between 0 and 1.[5,20] The configurational part of the pressure tensor from

Eq. (27) is

$$
\int_V \underline{\nabla} \cdot \underline{\underline{P}}^C(\underline{r}) dV = -\frac{1}{2} \left\langle \underline{\nabla} \cdot \sum_{i=1}^{N} \sum_{j \neq i}^{N} \frac{\underline{r}_{ij}\underline{r}_{ij}}{r_{ij}} \phi'_{ij}(r_{ij}) \int_0^1 \vartheta_\kappa(\alpha) d\alpha \right\rangle
$$

$$
= -\frac{1}{2} \left\langle \sum_{i=1}^{N} \sum_{j \neq i}^{N} \sum_{k=1}^{2} \frac{\underline{r}_{ij}\underline{r}_{ij}}{r_{ij}} \phi'_{ij}(r_{ij}) \cdot \frac{\hat{\underline{e}}_{n,k}}{|\underline{r}_{ij} \cdot \hat{\underline{e}}_{n,k}|} \left[H(\alpha_k) H(1 - \alpha_k) \right] \right\rangle
$$

$$
= -\frac{1}{2} \left\langle \sum_{i=1}^{N} \sum_{j \neq i}^{N} \sum_{k=1}^{2} \frac{\underline{r}_{ij}}{r_{ij}} \phi'_{ij}(r_{ij}) \mathrm{sgn}(\underline{r}_{ij} \cdot \underline{R}_k) \left[H(\alpha_k) H(1 - \alpha_k) \right] \right\rangle
$$

$$
= \oint_S \underline{\underline{P}}^C(\underline{r}) \cdot d\underline{S}. \tag{39}
$$

The penultimate line in the above set of equations is the formula for the configurational part of the traction in the radial extension of MOP. From the surface average relationship, $\oint_S \underline{\underline{P}}^C(\underline{r}) \cdot d\underline{S} \equiv A \underline{P}_{MOP}^C(R)$ then the total pressure tensor (more specifically tractions) in the MOP formulation is

$$
\underline{P}_{MOP}(R) = \frac{1}{A} \left\langle \sum_{i=1}^{N} \frac{1}{m_i} \underline{p}_i \underline{p}_i \cdot \hat{\underline{e}}_n \delta(R - r_i) \right\rangle
$$

$$
- \frac{1}{2A} \left\langle \sum_{i=1}^{N} \sum_{j \neq i}^{N} \sum_{k=1}^{2} \frac{\underline{r}_{ij}}{r_{ij}} \phi'_{ij}(r_{ij}) \mathrm{sgn}(\underline{r}_{ij} \cdot \underline{R}_k) H(\alpha_k) H(1 - \alpha_k) \right\rangle, \tag{40}
$$

where the first term on the right of Eq. (40) is the kinetic component of the pressure tensor, obtained by substituting Eqs. (29) in (27). Equation (40) will be referred to as the Radial Method of Planes (RMOP) formula. The formulas in Eq. (41) converge to the planar MOP formulas from Eq. (25), $P_{MOP}^{zz}(z)$ and $[P_{MOP}^{xz}(z) + P_{MOP}^{yz}(z)]/2$ as $R/\sigma \rightarrow \infty$ for molecules with molecular diameter, σ. The RMOP expressions in Eq. (40) are shown in Sec. II F to govern the evolution of momen-

tum in a control volume by *exactly* satisfying Eq. (21). The local pressure tensor is known to be non-unique;[22] however, this demonstration of the link between RMOP on the surface of a volume and the change of momentum inside it suggests this is the most physically meaningful formulation to use for the pressure tensor of a spherical subvolume.

The RIK form of pressure tensor assuming spherical symmetry is for the normal component, $\underline{P}_{MOP} \cdot \hat{\underline{e}}_n$,

$$
\underline{P}_{MOP,N}(R) = \frac{1}{A} \left\langle \sum_{i=1}^{N} \frac{1}{m_i} (\underline{p}_i \cdot \hat{\underline{e}}_n)^2 \delta(R - r_i) \right\rangle
$$

$$
- \frac{1}{2A} \left\langle \sum_{i=1}^{N} \sum_{j \neq i}^{N} \sum_{k=1}^{2} \frac{\underline{r}_{ij} \cdot \hat{\underline{e}}_n}{r_{ij}} \phi'_{ij}(r_{ij}) \mathrm{sgn}(\underline{r}_{ij} \cdot \underline{R}_k) H(\alpha_k) H(1 - \alpha_k) \right\rangle, \tag{41}
$$

and the tangential component is $(\underline{P}_{MOP} \cdot [\hat{\underline{e}}_{t_1} + \hat{\underline{e}}_{t_2}])$,

$$
\underline{P}_{MOP,T}(R) = \frac{1}{2A} \left\langle \sum_{i=1}^{N} \frac{1}{m_i} [\underline{p}_i \cdot \hat{\underline{e}}_{t_1} + \underline{p}_i \cdot \hat{\underline{e}}_{t_2}] \underline{p}_i \cdot \hat{\underline{e}}_n \delta(R - r_i) \right\rangle
$$

$$
- \frac{1}{4A} \left\langle \sum_{i=1}^{N} \sum_{j \neq i}^{N} \sum_{k=1}^{2} [\underline{r}_{ij} \cdot \hat{\underline{e}}_{t_1} + \underline{r}_{ij} \cdot \hat{\underline{e}}_{t_2}] \frac{\phi'_{ij}(r_{ij})}{r_{ij}} \mathrm{sgn}(\underline{r}_{ij} \cdot \underline{R}_k) H(\alpha_k) H(1 - \alpha_k) \right\rangle, \tag{42}
$$

respectively. For isotropic equilibrium conditions, $\underline{P}_{MOP,T}(R) = 0$ for reasons of symmetry. The behavior of the RIK and RMOP formulas in the $R \to 0$ limit is in part obtainable from general definitions, when combined with an analysis of the local distribution of molecules with respect to the sphere. The tangential component of the pressure tensor in Eq. (42) is an off-diagonal element, and is statistically zero at equilibrium. Whereas the corresponding RIK term in Eq. (14) is a diagonal element, and so is not zero on average. This can be seen also by taking the $R \to \infty$ limit where these expressions go over to the corresponding planar formulas of Ref. 26.

F. Evaluating the pressure tensor using the roots of a quadratic equation

The configurational part of the VA pressure tensor, Eq. (24), through $\ell_{ij} = \ell_{ij}(\alpha_k)$ includes a Heaviside function whose argument incorporates a quadratic with two roots, α_k. Similarly, for the RIK/MOP configurational pressure component, Eq. (39),

$$\oint_S \underline{\underline{P}}^C(\underline{r}) \cdot d\mathbf{S} = -\frac{1}{2} \left\langle \sum_{i=1}^{N} \sum_{j \neq i}^{N} \sum_{k=1}^{2} \frac{r_{ij}}{r_{ij}} \phi'_{ij}(r_{ij}) \right.$$
$$\left. \times \text{sgn}(\underline{r}_{ij} \cdot \underline{R}_k) \left[H(\alpha_k) H(1 - \alpha_k) \right] \right\rangle,$$
(43)

where again it is the roots of the intersection, α_k, which are key to evaluating the radial version of the MOP pressure tensor. In order to evaluate this root, there are three distances and three angles which when combined can be used to define the geometry of the two molecules, the center of the sphere, and the points of intersection, α_k, of $\underline{r}_{ij}$ with the surface of the sphere. These are annotated on the schematic diagram in Fig. 1. The three vectors are (a), $\underline{a} = \underline{r}_i - \underline{r}_0$, where $\underline{r}_0$ is the vector to the center of the sphere, (b) $\underline{b} \equiv \underline{r}_{ji} = \underline{r}_j - \underline{r}_i$, and (c) $\underline{R}$, the vector from the center of the sphere to where (if) $\underline{r}_{ji}$ crosses the surface of the sphere at point P. The angle between $\underline{a}$ and $\underline{b}$ is $\phi = \cos^{-1}[\underline{a} \cdot \underline{b}/ab]$. The other two angles of importance are θ which is the angle between $\underline{b}$ and $\underline{R}$ (i.e., $\theta = \cos^{-1}[\underline{R} \cdot \underline{b}/Rb]$, and β which is the angle between $\underline{a}$ and $\underline{R}$ (i.e., $\beta = \cos^{-1}[\underline{a} \cdot \underline{R}/aR]$). The vector, $\underline{l} = \underline{a} + \alpha \underline{b}$ defines the line along the molecule pair separation vector with the origin at the center of the sphere. The crossing point of $\underline{l}$ with the surface of the sphere is determined from $(\underline{a} + \alpha\underline{b})^2 = R^2$, which after solving the quadratic in α yields

$$\alpha_k = (a/b)\cos(\theta + \beta) \pm \sqrt{(R/b)^2 - (a/b)^2\sin^2(\phi)}. \quad (44)$$

The physical interpretation of the various roots of this equation is discussed in Appendix B.

Equation (44) is directly dependent on all three angles β, θ, ϕ and the magnitude of the lengths of the various vectors a, b, R. The variation of the pressure tensor as a function of sphere radius R is of particular interest, all other parameters being intrinsic functions of the system. The probability distribution of these angles as a function of the sphere radius helps interpret the effects of local structural arrangements of
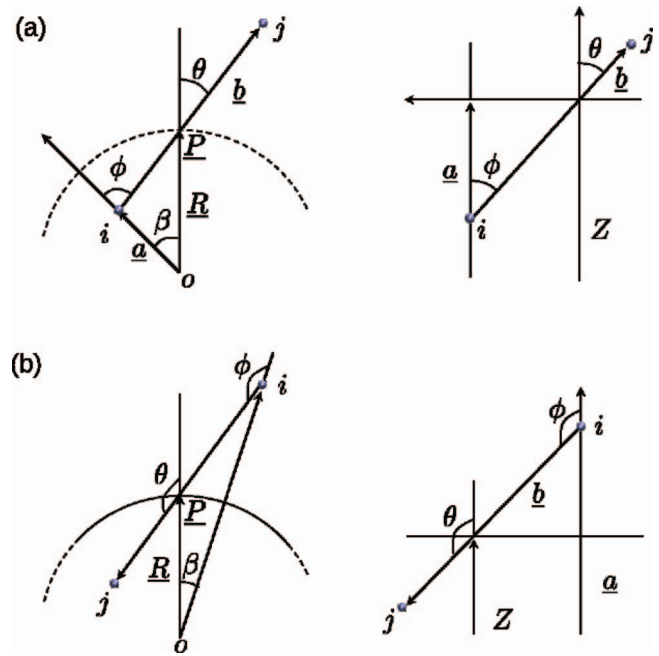

FIG. 1. Schematic diagram of the angles and vectors which define the relationship between the two interacting molecules, i and j and the sphere of radius, R (see also Appendix A). The top left frame is for the sphere when i is inside and j is outside the sphere. (a) The top right frame is the limit of $R \to \infty$ to give a planar boundary. (b) The bottom two frames correspond to the same situations but with i outside the sphere and j inside it.

molecules on the pressure tensor as $R \to 0$ and $R \to \infty$. The R dependence of the angles in Eq. (44) is explored in Sec. III in order to quantify the sub-volume sizes necessary to converge particular observables and to explore the implications for the underlying physics.

Two types of spherical control volume are considered, one where the origin is placed randomly in the liquid, which corresponds to the starting point of Irving and Kirkwood in their paper. The other case is where the origin of the sphere coincides with the center of one of the molecules, corresponding to the form used by Irving and Kirkwood in terms of the radial distribution function both for the whole system in the main text and over a local surface in the Appendix of that paper. The definition of a local stress or pressure tensor centered on a single atom or molecule is a longstanding construction in the literature (see, for example, IK1 in Refs. 13 and 29) and on physical grounds is perhaps the natural origin to choose for a local pressure tensor as molecular interactions represented by pair potentials which originate from such points. Indeed, Zhou[38] argued that molecular pressure can only be defined at the location of a molecule in a molecular system. The advantage of having a molecule at the center of the control volume is that the local stress could be measured by spectroscopic experiments.[30] Although not the focus of this work, in the solid continuum-atomistic coupling literature, often the local stress is implicitly assumed to be atom-centric in order to couple to the nodes in the continuum description.[31,32] Differences between the local pressure tensor from the two definitions will also help to identify the consequences of nearby-molecule packing constraints on this quantity.
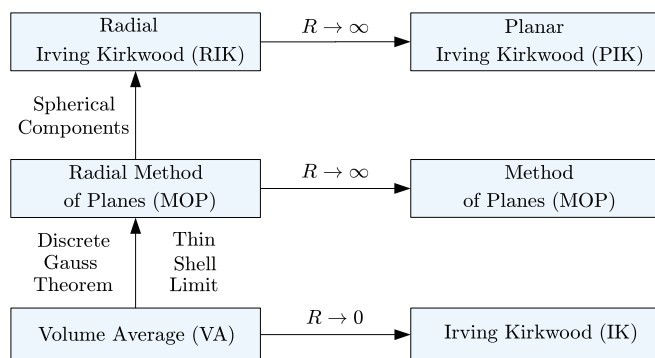
FIG. 2. Schematic diagram relating the various expressions for the radial and planar limit definitions of the local pressure tensor.

The relationships between the various definitions of the pressure tensor for the spherical and planar limits presented in this section are given schematically in Fig. 2.

III. RESULTS AND DISCUSSION

Molecular Dynamics (MD) simulations have been carried out using the isotropic repulsive Lennard-Jones or Weeks-Chandler-Andersen (WCA) potential, $\phi(r) = 4\epsilon[(\sigma/r)^{12} - (\sigma/r)^6] + 1$, $r \leq 2^{1/6}$; $= 0$, $r > 2^{1/6}$, where ϵ and σ define the energy and length scales, respectively. The truncation distance of the pair interactions was $r_c = 2^{1/6}$. All atoms in the system have the same mass, m, and the reduced temperature is defined to be $T^* = k_B T/\epsilon = 2$ (the asterisk being omitted in subsequent discussion). The reduced density was $\rho = 0.6$ and the reduced time step was 0.00354.

Figure 3 shows the various terms of the conservation of momentum equation, Eq. (21) computed for a single arbitrary spherical volume of radius 3.0. The terms in the momentum equation, Eq. (21), include "Advection", the magnitude of RMOP kinetic pressure and convection, $|\underline{P}_{MOP}^K|$

$+ \oint \rho \underline{u}\underline{u} \cdot d\underline{S}$, which is zero until molecules cross the surface, then has a peak equal to the momentum of the molecule entering the spherical CV. The "Forcing" term is the magnitude of the RMOP configurational pressure, $\underline{P}_{MOP}^C$ and is equal to the sum of the forces acting over the surface of the sphere. Finally, the "Accumulation" terms is the magnitude of the time evolution in the sphere $d/dt \sum_{i=1}^{N} |m_i v_i|$ at each time step. The figure verifies that the definition of the RMOP in Eq. (40) satisfies continuity as the Residual ("Residual = Accumulation − Forcing + Advection") in Fig. 3 is zero to machine precision in a molecular simulation. This establishes the direct link between the configurational and kinetic components of RMOP on the sphere surface to the time evolution of the momemtum inside that sphere. The exact agreement is only possible using the RMOP pressure tensor definition, which requires an exact calculation of the location of the crossing of the interaction and molecules at each timestep.

The data in the remaining figures are derived from a $N = 4000$ simulation of 2×10^5 time steps. The centers of 100 randomly chosen molecules were used as the origins of the spherical volumes. Two types of simulation were carried out, the first where there was a molecule at the center of the sphere of radius R (the "C" case), and the second where the sphere was placed randomly in the simulation cell (the "N" case).

The three angles, θ, ϕ, and β in Fig. 1, together with the spherical radius R, define the location of the roots α_k. These roots determine the VA stress (see Eq. (24)) through ℓ_{ij} in Eq. (17) as well as the MOP stress in Eq. (40). These angles are therefore of central importance to the sphere-radius dependence of the local pressure tensor whose statistics are explored in this section. The probability distribution of θ, ϕ, and β is evaluated in Figs. 4–6, respectively. Next, the behavior of the average values of these angles as a function of radius, R, is explored in Figs. 7–9, respectively. The combination of these three angles define the resulting inter-molecular interaction inside the volume, ℓ_{ij}, which is presented as a function of R in Fig. 10. Finally, the stress tensor itself is presented as a function of R in Fig. 11.

The probability distribution functions of the three key angles are generated from those pair interactions between

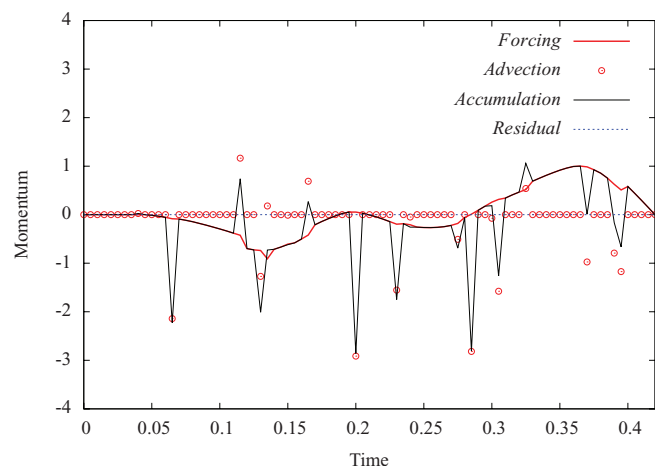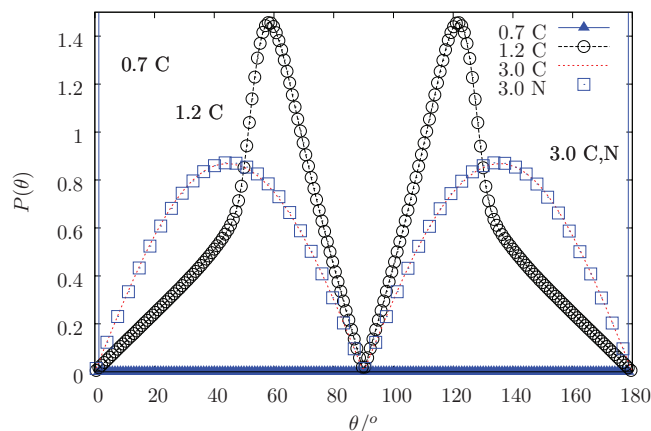
FIG. 3. Momentum balance for a spherical volume of radius 3.0 over a simulation time of 0.42 MD units (see Eq. (21). Terms of Eq. (21) are plotted at each time together with their "Residual = Accumulation − Forcing + Advection", is shown to be equal to zero throughout, as it should be from Eq. (21)).

FIG. 4. $P(\theta) \times 100$ for spheres centered on arbitrary molecules for radii, R = 0.7, 1.2, and 3.0 denoted by "C" in the figure. Also shown is $R = 3.0$ for the case where the center of the sphere is chosen randomly in the MD cell ("N" on the figure).
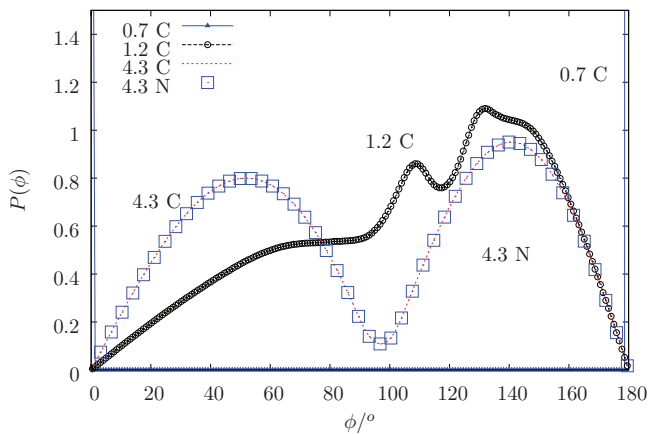
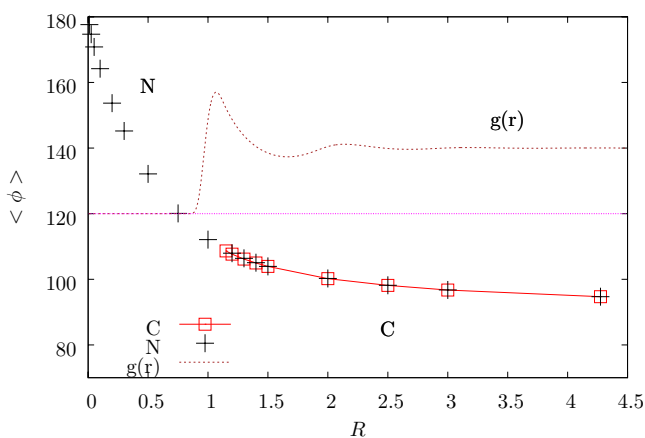FIG. 5. As for Fig. 4, except $P(\phi) \times 100$ is shown.

FIG. 8. As for Fig. 7, except the average of the angle, ϕ, indicated in Fig. 1, is shown. The radial distribution function, $g(r)$, is multiplied by 20 and shifted upwards by 120.
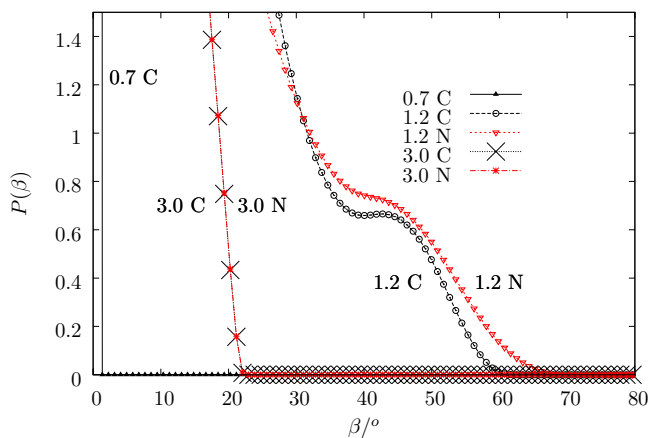

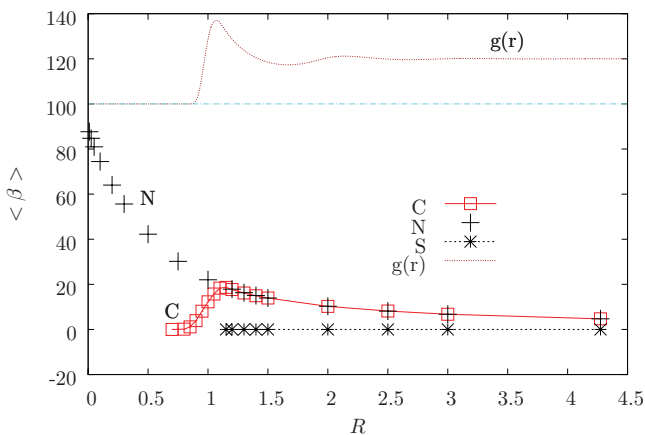FIG. 6. As for Fig. 4, except $P(\beta) \times 100$ is shown.

FIG. 9. As for Fig. 7, except the average of the angle, β, indicated in Fig. 1, is shown. The radial distribution function is shifted upwards by 100 and multiplied by 20. The quantity "S" on the figure is $\theta - \phi + \beta$ for the C simulation.
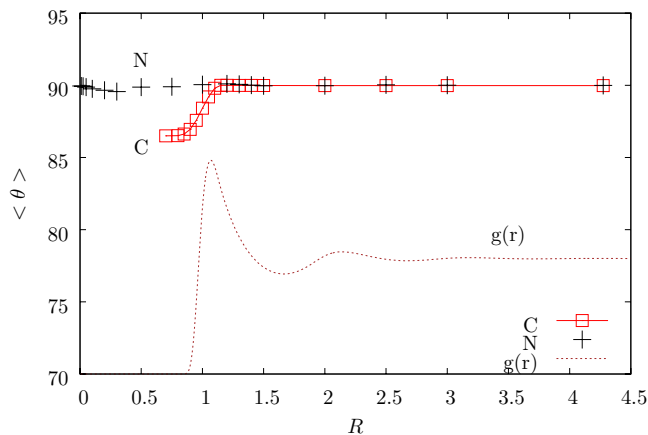

FIG. 7. The average of the angle θ indicated in Fig. 1, as a function of the sphere radius, R. "C" is the case where there is a molecule at the center of the sphere, and "N" is where the center of the sphere is positioned randomly in the simulation cell. The radial distribution function, $g(r)$ (multiplied by 8 and shifted upwards by 70), is also shown on the figure.
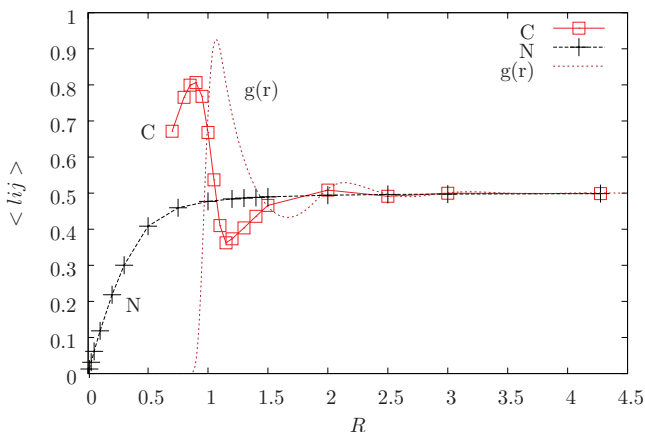

FIG. 10. As for Fig. 7, except the average of ℓ_{ij} is shown. The radial distribution function is multiplied by 0.5.
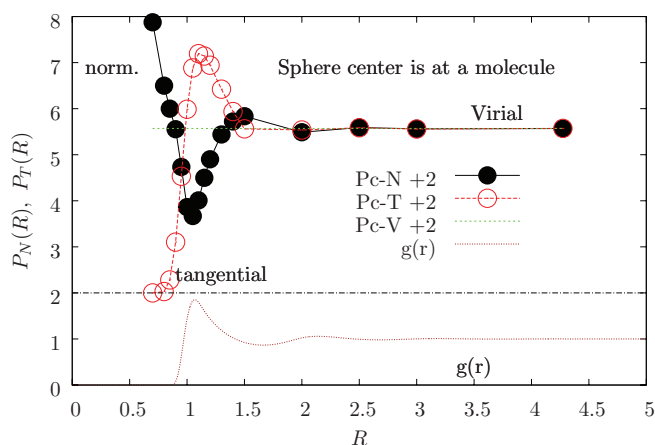
FIG. 11. Key: (a) The R-dependence of the interaction part RIK normal part of the pressure tensor, $P_N^c(r)$ from Eq. (13) labeled as "Pc-N," which is the same as the corresponding RMOP formula, and (b) the R-dependence of the interaction part of the RIK tangential part of the pressure tensor, $P_T^c(r)$ from Eq. (14) labeled as "Pc-T." (c) The R-dependence of the interaction part of the bulk pressure from the virial expression of Eq. (1). These three quantities are shifted upwards by 2. There is a molecule at the center of the sphere. The (unscaled) radial distribution function is shown also.

molecules, i and j, where the line between their centers crosses the surface of the sphere at least once. The probability distribution of angle θ, or $P(\theta)$, for example, is defined as

$$P(\theta_n) = N(\theta_n)/\Delta\theta \sum_{m=1}^{M} N(\theta_m), \qquad (45)$$

where $N(\theta_n)$ is the number of occurrences of θ in the interval $\theta_n \pm \Delta\theta/2$, where $\Delta\theta = 360°/M$ and $M = 400$. The corresponding distributions for the angles ϕ and β are defined in the same way.

Figure 4 shows $P(\theta)$ for spheres centered on arbitrary molecules (C-case) for radii, $R = 0.7$, 1.2, and 3.0, and another for $R = 3.0$ where the sphere is positioned randomly in the MD cell (the N-case). The values of radius are chosen to evaluate interactions within the excluded volume ($R = 0.7$), just outside the cutoff length $R = 1.2$ and an arbitrarily large radius $R = 3.0$. The distribution is symmetric about $\theta = 90°$, and tends to zero as $\theta \to 90°$ for all R, as this angle corresponds to the situation where $\underline{r}_{ij}$ is tangential to the surface, whose probability tends to 0 at this limiting angle. For large R, the distribution peaks at $45°$ and $135°$, which is the most probable value based on unbiased statistics. The C and N distributions are statistically indistinguishable for *ca.* $R \geq 3$. The sum of the θ when i and j are swapped equals $180°$ for all R which explains the symmetry of this function about $\theta = 90°$ for all R. As R decreases to ~ 1, excluded volume interactions in the C case strongly affects the form of $P(\theta)$. There are peaks near $60°$ and $120°$, and "spikes" in $P(\theta)$ at $0°$ and $180°$ (which are finite in width in the figure because of the finite width of the histogram bins). The former aspect arises because atoms i, j, and the one at the origin tend to form an equilateral triangle for $R \sim 1$. The two spikes are where molecule i is at the center of the sphere, the only physically possible case for very small

R in the C class of virtual sphere as a result of the excluded volume interactions.

For the probability distribution functions of the other angles it is useful to use the exact relationship for all $\underline{r}_{ij}$ which cross the sphere's surface, that $\phi = \theta + \beta$ for all R in the molecule centred (C) and random centred (N) classes of sphere. In the $R \to \infty$ limit where $\beta \to 0$ (see the left hand "planar limit" frames in Fig. 1) then $P(\phi)$ should tend to $P(\theta)$. The sphere surface approaches a flat plane geometry on the scale of a few molecules. In this limit $\phi \to \theta$ for all ij pairs which cross the surface of the sphere. The function, $P(\phi)$ shown in Fig. 5 reveals that convergence to $P(\theta)$ is slow with R however, as the limit $\beta \to 0$ is itself slow to converge with increasing R (see below). The distribution is anisotropic and there are two peaks at *ca.* 60 and 150° for $R = 3.0$. The sum of the two values of ϕ when i and j are swapped does not equal 180° (unlike the case for θ), but depends on β, and only when $\beta \to 0$ will $P(\phi)$ tend to $P(\theta)$ in the large R limit. There is significant structure in $P(\phi)$ when $R \sim 1$ and takes on smaller values. A general feature for the C class of sphere is that $P(\phi)$ becomes less symmetrical about 90° as R decreases.

The appearance of $P(\beta)$ given in Fig. 6 is quite different to the other two angle distributions. With increasing sphere radius the distribution of β shifts progressively to becoming a sharp peak at $\beta = 0$, which can be appreciated from the right hand frames in Fig. 1. There is also a peak at $\beta = 0$ in the distribution for small $R \ll 1$ for the C class of virtual sphere. In the limit $R \to 0$, molecule i has to be at the center of the sphere for there to be a surface crossing of the ij separation vector at all; in this case β must equal 0.

Figure 7 shows the R-dependence of the average value of the angle θ for those molecule pairs whose separation vector crosses the surface of the sphere. In the large R limit, the mean of θ, denoted by $\langle\theta\rangle$, is 90° for both C and N type of spheres. However, for the C case, the mean drops below 90° in the vicinity of the first peak in $g(r)$, because only i can be at the center of the sphere (θ is defined with respect to the vector from the center to i) so this shifts the mean of θ to angles less than 90°. There are no points in the radial distribution function for $r < 0.82$ for this MD system but it is expected that $\langle\theta\rangle$ would go to zero in the $R \to 0$ limit. For the N-type of virtual sphere the mean angle of θ is 90° for all R. In the $R \to 0$ limit there will not be any molecules inside the sphere, therefore all interactions are due to interactions between external molecules crossing the sphere. For external molecules there are two crossings of r_{ij} with the sphere, and as $\theta_1 + \theta_2 = 180°$, the average tends to 90°.

The mean of ϕ, denoted $\langle\phi\rangle$, as a function of R is shown in Fig. 8. For the N type of sphere, $\langle\phi\rangle$ decreases slowly from 180° in the $R \to 0$ limit to 90° as $R \to \infty$. In the $R \to 0$ limit then $\langle\phi\rangle$ tends to 180° and as $R \to \infty$ it may be seen that $\langle\phi\rangle$ tends to 90°, as expected by inspection. The C and N curves coincide for $R > 1$ but $\langle\phi\rangle$ will tend to zero as $R \to 0$ limit in the C case. For the C class of sphere, $\langle\phi\rangle$ drops rapidly to zero for $R < 1$, as then only when i is the central molecule is there an ij contribution (in this case $\phi = 0$).

The mean of β, denoted $\langle\beta\rangle$, as a function of R is shown in Fig. 9. In the N case, $\langle\beta\rangle \rightarrow 90°$ as $R \rightarrow 0$ because of the two possible crossings, one will have $\beta = 0°$ and the other $\beta = 180°$. As the $\langle\theta\rangle$ component is constant for the N case, the $\langle\beta\rangle$ will change as a function of R in an identical manner to $\langle\phi\rangle$ as $\phi = \theta + \beta$. In the C case, $\langle\beta\rangle$ drops to zero within the first peak in the radial distribution function. This is a consequence of molecule i increasingly being the central molecule as R decreases below unity, which forces β to be zero when that occurs. Figure 9 also shows that $\langle\beta\rangle$ decreases quite slowly to zero as $R \rightarrow \infty$. Because of excluded volume effects there are no values of θ, ϕ, and β below a certain value of $R < 1$; nevertheless from the fact that i must be the central molecule in the small R limit it can be concluded that all these angles must tend to zero when this limit is taken.

Figure 10 shows the mean value of ℓ_{ij} or $\langle\ell_{ij}\rangle$ as a function of R. For the N type of sphere, $\langle\ell_{ij}\rangle$ increases monotonically from 0 at $R = 0$ to 1/2 by $R \approx 2$. The C class of sphere has a different behavior for small R, particularly for $R \sim 1$, which correlates well with the first peak in the radial distribution function. Between $R = 1$–1.5, $\langle\ell_{ij}\rangle$ for type C sphere is below the N value, and for $R < 1$ the reverse trend is evident. As R decreases through the first peak, the configurations where i and the central molecule are the same dominate, so with diminishing R there is a transition from a bias of tangential to normal crossings (where l_{ij} will be larger than its limiting value as $R \rightarrow \infty$).

Figure 11 shows the R-dependence of the normal and tangential components of the RIK version of the configurational part of the pressure tensor, defined in Eqs. (13) and (14), respectively. This figure is for the C class of sphere. They converge to the virial formula value from Eq. (1) by $R \approx 2$ and for larger R. This is perhaps not surprising as the virial expression for the pressure tensor can be rearranged to be equal to the pair forces crossing the cell boundaries between a molecule inside the cell and the periodic image of another molecule (i.e., the MOP definition). For the C category of sphere, differences between P_N and P_T are apparent for R less than about 2σ, and the features correlate well with those of the first peak in $g(r)$. For small R the tangential component increases before decreasing to zero for $R \simeq 0.85$. The increase in P_T is probably because r_{ij} is typically near tangential to the surface of the sphere in this distance range. The $|\underline{r}_{ij}.\hat{\underline{e}}_{n,k}|$ terms in the denominator in Eq. (14) will be small, a feature which accentuates these contributions, and gives values of P_T above the large R limit. As R becomes even smaller, only the cases where i is at the center of the sphere contribute to the pressure tensor, which is why P_T decreases quickly to zero for even smaller R (fewer tangential crossings). The normal value, P_N, increases probably because the surface area, $A(R)$, decreases with R, and the typical $\underline{r}_{ij}$ is normal to the surface of the sphere in this limit. The corresponding data for the N class of sphere shows that P_N and P_T agree with the virial results for all R. In the limit, $R \rightarrow 0$ the data points are noisy due to the relatively small number of surface crossings in this limit. The independence of $P_N(R)$ and $P_T(R)$ with R for the RIK formulas shows in a practical way that the RIK formula in the N class reduces to the Irving-Kirkwood definition of the pressure tensor at a

point (i.e., $R = 0$ here), when the sphere approaches the zero volume limit.

Fluctuation-based quantities calculated by molecular simulation in a defined volume have been of interest for some time, for example, as a route to second order thermodynamic quantities,[33] and transport coefficients (using the Green-Kubo time correlation function formulas[21]), and the fluctuation theorem applied to small subsystems.[34] Recently, there has been renewed interest in these type of quantities in the context of hydrodynamic flows,[35] and MD-Continuum coupling for fluids.[36] An example of a physically meaningful fluctuation quantity is the infinite frequency shear rigidity modulus of a bulk fluid, which is defined as $G_\infty = V_{sim}\langle P_{xy}^2\rangle/k_BT$, where V_{sim} is the volume of the MD simulation cell and P_{xy}, an off-diagonal element of the pressure tensor obtained from the virial formula of Eq. (1). This quantity measures the initial "elastic" or solid-like response of a liquid when subjected to a suddenly implemented step in shear strain applied affinely to all the molecules in the system. G_∞ has been found to be relatively insensitive to N, for not too small values of this number. The corresponding quantity for a finite subvolume within a MD cell can also be defined as $G_\infty^{VA} = \Omega\langle P_{xy}^2\rangle/k_BT$, using the VA measure of the average local pressure tensor within a spherical subvolume, $\Omega(R)$, for radius R. Only the $R \rightarrow \infty$ limit has physical significance, but nevertheless it is of interest to explore the convergence rate with R to this limit, and how the total number of molecules in the simulation cell affects the trend towards the value in the thermodynamic limit. It would be expected that for sufficiently large R the two expressions, G_∞ and G_∞^{VA} should converge, which is seen to be the case in Fig. 12. Figure 12 presents these two quantities obtained by MD simulation for the WCA state point, $\rho = 0.7$ and $T = 2.0$. The center of the sphere is placed in the middle of the simulation cell. The number of molecules in the simulation cell
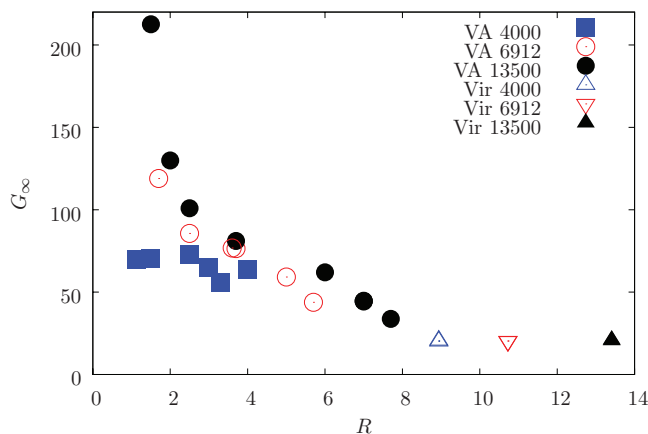

FIG. 12. The dependence of the mean square shear stress, $\Omega\langle P_{xy}^2\rangle/k_BT$ calculated using the VA method ("VA"), where R is the radius of the sphere and Ω is its volume. The simulation parameters are, $\rho = 0.7$ and $T = 2.0$ for a WCA molecule MD simulation. The number of molecules in the unit cell is given in the key on the figure. The center of the sphere is placed in the middle of the simulation cell. The infinite frequency shear rigidity modulus, $G_\infty = V_{sim}\langle P_{xy}^2\rangle/k_BT$ are also shown ("Vir") where V_{sim} is the volume of the cubic unit cell, applied to $N = 4000$, 6912, and 13500 molecule systems, and this time, P_{xy} is the xy element of the pressure tensor by the virial formula from Eq. (1). For the virial stress fluctuations, which includes all of the interactions in the cubic cell, R is replaced by half the MD cell's sidelength.

is given in the key on the figure. It is noticeable that for this state point the convergence in $G_\infty^{VA}(R)$ is quite slow, requiring a sphere radius of $R \simeq 10$ before convergence is achieved to an acceptable extent. The other feature of note is that the fluctuations for a given R are strongly sensitive to N, the total number of molecules in the simulation cell. As N decreases, the mean square P_{xy} diminishes for a given R. The general trend for any given value of N is for $G_\infty^{VA}(R)$ to increase with diminishing R. As $R \leq S/2$, where S is the sidelength of the cubic MD cell, quite large systems are required to obtain G_∞ using a spherical subvolume, which will also depend on the state point.

The shear stress fluctuations in a subvolume can be decomposed into 2-, 3-, and 4-body components. The relative importance of these will depend on the size and shape of the subvolume. The 3-body is of opposite sign to the 2 and 4 body, so the final value of stress fluctuation is the relatively small difference between two large numbers.[37] It is not just a surface or "surface crossing" effect but what is contained, or can be fitted into the sphere of given radius that is also important. This is why we expect the quantity plotted in Fig. 12 to be particularly R- and total N-dependent. Figure 12 shows that the magnitude of the variance in quantities within a subvolume in a typical MD simulation, quite generally, depends strongly on the size of the subvolume and also that of the simulation cell (this will also apply to any corresponding Monte Carlo simulation), and can be slow to converge with control volume radius. Fluctuation-derived second order thermodynamic quantities are known to be particularly sensitive to system size in MD simulation in comparison to the corresponding first order thermodynamic properties.

IV. CONCLUSIONS

This work has extended previous treatments of the local pressure tensor at a plane to the case of the boundary of a virtual sphere in a bulk system. The MOP approach of Todd *et al.*[13] has been developed to apply to a virtual spherical surface using the CV formulation of Smith *et al.*[20] The radial component of the MOP pressure tensor reduces to the corresponding RIK expression which has been used since at least the 1980s for molecular simulation of droplets and other curved interfaces, but applies equally well as a measure of the local stress within a virtual spherical subvolume in a bulk system. The MOP definition of the stress over any enclosed surface exactly equals the momentum changes of the volume within. In Ref. 20, the volume is a cube and the MOP description over the six surfaces ensures momentum conservation, while in the spherical case, the MOP solution over the spherical surface exactly equals the momentum change in the sphere. It is for this reason that the RMOP form of pressure tensor provides exact conservation and the other forms, such as VA, do not.

The various formulas for the radial-dependent pressure tensor converge in the infinite radius limit to their planar boundary counterparts which have been derived elsewhere. Molecular dynamics simulations of bulk fluids provide some insight into the rate of convergence with the radius of the sphere, and the deviations in behavior from the macroscopic

limit when the radius is of order the molecular diameter. If the sampling sphere is positioned randomly or at a fixed location in the simulation cell the normal and tangential components of the pressure tensor are within statistics independent of sphere radius, R. If there is a molecule at the center of the sphere the radial or R-dependent pressure profiles are affected by excluded volume effects for sphere radii of order the molecular diameter and the trends correlate well with the peaks in the radial distribution function. As discussed in Sec. III, there are situations where it is most appropriate to have either a molecule or atom at the center of the sphere, or to fix the center in space. The latter case would especially apply for a fluid near a solid wall, where the virial formula is not applicable.

The behavior of the local pressure tensor for R of order the diameter of the molecule is affected by the excluded volume interactions between those molecules within the sphere and those which cross its boundary. The probability distribution of three key angles entering into the local geometry description has been computed by MD. The behavior of these distributions can be interpreted for large R by inspection largely in terms of symmetry considerations, and for R of order one molecular diameter and smaller, in terms of excluded volume effects which lead to certain dominant arrangements of two or three molecules. There is a transition from predominantly tangential to normal interactions as the sphere radius decreases within the first peak of the radial distribution function.

The variance of the stress in spherical subvolumes computed by the VA method was shown to converge slowly with radius, and particularly with system size.

ACKNOWLEDGMENTS

APPENDIX A: POINTS OF INTERSECTION, α_k, OF $\underline{r}_{ij}$ WITH THE SURFACE OF THE SPHERE

More details on how the intersection of the vector between molecules i and j with the surface of the sphere are obtained are discussed in this Appendix. For the VA pressure tensor, the molecules i and j whose line between their centers crosses the surface at least once, or is entirely within the spherical volume, contributes to the configurational part of the pressure tensor. From the crossing locations, α_k, the length of interaction inside a sphere is easily obtained. For the RIK or the MOP formulations only those pairs whose separation vector crosses the spherical surface contribute to the pressure tensor are relevant. "Virtual" crossings (i.e., $\alpha_k < 0$ or $\alpha_k > 1$) when both i and j are within the sphere are not included. If both solutions are real and $0 \leq \alpha_k \leq 1$, this indicates a crossing of the sphere's surface by the inter-molecular interaction vector $\underline{r}_{ij}$. The various solutions to this equation are
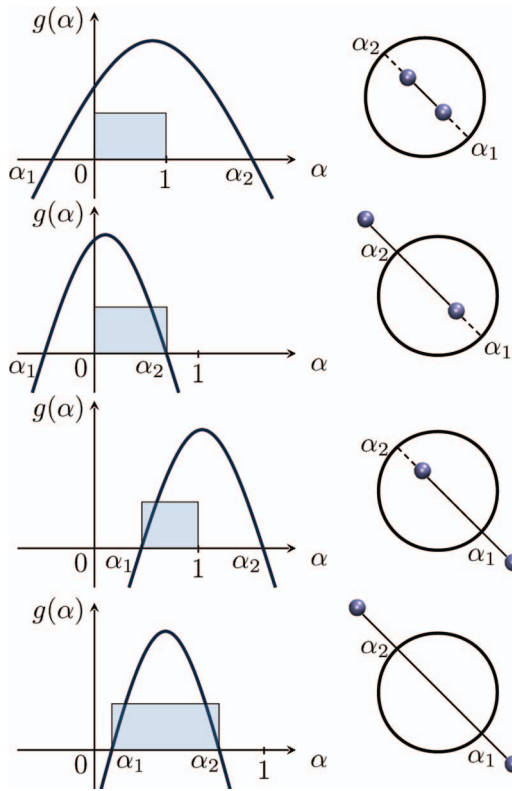
FIG. 13. Schematic diagram showing possible solutions of the sphere-line intersect equation inside the Heaviside function of Eq. (24) together with the cases which they represent. The various cases are described in Appendix A including both molecules inside (top figure, no intersection) and either i or j outside (middle and bottom figure, single intersect) or both outside.

shown in Fig. 13. If both solutions, α_1 and α_2 are complex, the pair i and j are both outside the sphere, and their separation vector does not cross the sphere, so that term does not contribute to Eqs. (24)–(43). If both molecules are inside the sphere, one value of α will be less than zero and the other will be greater than unity. The Heaviside function of Eq. (24) is always equal to unity and the integral along the whole line yields $\ell_{ij} = 1$. This is illustrated in the top frame in Fig. 13. If only $\underline{r}_i$ or $\underline{r}_j$ is inside the sphere then one of the solutions (say α_1) is bounded by $0 < \alpha_1 < 1$ and the other solution is less than zero or greater than 1 (see the middle two frames in Fig. 13). The integration is along the part of the line from the intersection, α_1, to the position of the molecule $\underline{r}_i$ inside so $0 < \ell_{ij} < 1$ based on this length. Alternatively, if both molecules are outside and the interaction crosses the volume twice as seen in the bottom frame. The fraction of the total interaction within the volume, α_1 to α_2, is included. As the internal angles of the triangle, iP0 of Fig. 1 must add up to π, then $\phi = \theta + \beta$.

APPENDIX B: THE VOLUME AVERAGING FORMULA FOR THE AVERAGE PRESSURE TENSOR FOR A THIN SPHERICAL SHELL

The VA formula for the pressure tensor associated with a thin shell of thickness Δr about radial position R is derived in this Appendix. The integral over a spherical shell volume

element, $dV = r^2 \sin\theta d\phi d\theta dr$ is

$$\vartheta_\kappa = \int_V \delta\left(\underline{r} - \underline{\tilde{r}}_\kappa\right) dV$$

$$= \int_{R_I}^{R_o} dr \int_0^\pi d\theta \int_0^{2\pi} d\phi \, \delta\left(r - r_\kappa\right) \delta\left(\theta - \theta_\kappa\right) \delta\left(\phi - \phi_\kappa\right)$$

$$= [H\left(R_o - r_\kappa\right) - H\left(R_I - r_\kappa\right)][H\left(\pi - \theta_\kappa\right) - H\left(-\theta_\kappa\right)]$$

$$\times [H\left(2\pi - \phi_\kappa\right) - H\left(-\phi_\kappa\right)]. \tag{B1}$$

Let R be the point mid-way between the outer radius R_o and the inner radius, R_I, so $R_o = R + \Delta R/2$ and $R_I = R - \Delta R/2$. The annulus has a thickness ΔR. The angles are confined, by convention, to the range, $0 < \theta < \pi$ and $0 < \phi < 2\pi$; therefore, the expression for the spherical shell CV in Eq. (B1) can be simplified to

$$\vartheta_\kappa = H\left(R_o - r_\kappa\right) - H\left(R_I - r_\kappa\right). \tag{B2}$$

The volume between the two radii is, $V_a = \pi \Delta R(R_o^2 - R_I^2)$. Using the definition of R_o and R_I the volume simplifies to $V_a = 2\pi R^2 \Delta R$ for $\Delta R/R \ll 1$. The VA stress tensor attached to the annular volume is

$$\underline{\underline{P}}_{VA}^k(V) + \underline{\underline{P}}_{VA}^c(V)$$

$$= \frac{1}{2\pi R^2 \Delta R} \left\langle \sum_{i=1}^N \frac{1}{m_i} \underline{p}_i \underline{p}_i \vartheta_i \right\rangle$$

$$- \frac{1}{4\pi R^2 \Delta R} \left\langle \sum_{i=1}^N \sum_{j\neq i}^N \frac{\underline{r}_{ij}\underline{r}_{ij}}{r_{ij}} \phi_{ij}'(r_{ij})\ell_{ij} \right\rangle, \tag{B3}$$

where $\ell_{ij} = \int_0^1 \vartheta_\kappa d\alpha$, and where $\vartheta_k = 1$ if r_k is in volume V_a and zero otherwise.

It is instructive to consider two limiting cases for Eq. (B3), the first is where the inner radius, R_I, tends to zero and the second is where the annular thickness, ΔR, tends to zero. In the first case the spherical VA from of stress given in Eqs. (23) and (24) can be reclaimed as

$$\lim_{R_I \to 0} \vartheta_\kappa = H\left(R_o - r_\kappa\right) - \lim_{R_I \to 0} H\left(R_I - r_\kappa\right) = H\left(R_o - r_\kappa\right) \tag{B4}$$

and $H(-r_\kappa) = 0$ for all r_κ.

In the limit of the annular volume in Eq. (B3) tending to zero thickness at point R, i.e., $\Delta R \to 0$, only the normal component ($\underline{\hat{e}}_n$) to the spherical surface is relevant

$$\lim_{\Delta R \to 0} \left[\underline{\underline{P}}_{VA}^k + \underline{\underline{P}}_{VA}^c\right] \cdot \underline{\hat{e}}_n$$

$$= \lim_{\Delta R \to 0} \left[\frac{1}{2\pi R} \left\langle \sum_{i=1}^N \frac{1}{m_i} \underline{p}_i \underline{p}_i \cdot \underline{\hat{e}}_n \frac{\vartheta_i}{\Delta R} \right\rangle \right.$$

$$\left. - \frac{1}{4\pi R} \left\langle \sum_{i=1}^N \sum_{j\neq i}^N \frac{\underline{r}_{ij}\underline{r}_{ij} \cdot \underline{\hat{e}}_n}{r_{ij}} \phi_{ij}'(r_{ij}) \frac{\ell_{ij}}{\Delta R} \right\rangle \right]. \tag{B5}$$

The limit for the CV function is[26]

$$\lim_{\Delta R \to 0} \frac{\vartheta_\kappa}{\Delta R} = \frac{1}{\Delta R} \left[H\left(R + \frac{\Delta R}{2} - r_\kappa\right) - H\left(R - \frac{\Delta R}{2} - r_\kappa\right) \right] = \delta(R - r_\kappa). \quad (B6)$$

Similarly, the limit for the interaction between two molecules, ℓ_{ij}, is evaluated using

$$\lim_{\Delta R \to 0} \frac{\ell_{ij}}{\Delta R} = \lim_{\Delta R \to 0} \frac{\int_0^1 \vartheta_\kappa(\alpha) d\alpha}{\Delta R}$$

$$= \int_0^1 \delta(R - r_\kappa(\alpha)) d\alpha$$

$$= \sum_{k=1}^2 \frac{1}{|\underline{r}_{ji} \cdot \hat{\underline{e}}_{n,k}|} \left[H(1 - \alpha_k) - H(-\alpha_k) \right],$$

$$(B7)$$

where the final equality follows from Eq. (38). Substitution of Eq. (B7) in (B5) yields the MOP form of pressure tensor. The evaluation of the zero-volume limit of an annulus is mathematically identical to evaluating the derivative as in Eq. (39) in Sec. II E. Therefore, in the $\Delta R \to 0$ limit the VA and RMOP radial or normal pressure tensor components are mathematically equivalent for a subvolume sphere of radius R. They go over to the corresponding planar interface formulas,[26] in the large R limit. Consequently, the underlying relationships between the VA and MOP stresses for planar boundaries discussed in Refs. 20 and 26 and these spherical subvolume formulas have been established.

[1] J. H. Irving and J. G. Kirkwood, J. Chem. Phys. **18**, 817 (1950).
[2] M. Rao and B. J. Berne, Mol. Phys. **37**, 455 (1979).
[3] J. P. R. B. Walton and K. E. Gubbins, Mol. Phys. **55**, 679 (1985).
[4] A. P. Shreve, J. P. R. B. Walton, and K. E. Gubbins, J. Chem. Phys. **85**, 2178 (1986).
[5] G. J. Tjatjopoulos and J. Adin Mann, Mol. Phys. **60**, 1425 (1987).
[6] B. Hafskjold and T. Ikeshoji, Phys. Rev. E **66**, 011203 (2002).
[7] T. Ikeshoji, B. Hafskjold, and H. Furuholt, Mol. Sim. **29**, 101 (2003).
[8] T. Nakamura, W. Shinoda, and T. Ikeshoji, J. Chem. Phys. **135**, 094106 (2011).
[9] A. J. Sodt and R. W. Pastor, J. Chem. Phys. **137**, 234101 (2012).
[10] R. J. Hardy, J. Chem. Phys. **76**, 622 (1982).
[11] J. F. Lutsko, J. Appl. Phys. **64**, 1152 (1988).
[12] J. Cormier, J. M. Rickman, and T. J. Delph, J. Appl. Phys. **89**, 99 (2001).
[13] B. D. Todd, D. J. Evans, and P. J. Daivis, Phys. Rev. E **52**, 1627 (1995).
[14] D. J. Evans and G. Morriss, *Statistical Mechanics of Nonequilibrium Liquids*, 2nd ed. (Cambridge University Press, 2008).
[15] F. Varnik, J. Baschnagel, and K. Binder, J. Chem. Phys. **113**, 4444 (2000).
[16] A. P. Thompson, J. Chem. Phys. **119**, 7503 (2003).
[17] J. M. Rodgers, C. Kaur, Y. G. Chen, and J. D. Weeks, Phys. Rev. Lett. **97**, 097801 (2006).
[18] C. Liu and Z. Li, Phys. Rev. Lett. **105**, 174501 (2010).
[19] D. H. Tsai, J. Chem. Phys. **70**, 1375 (1979).
[20] E. R. Smith, D. M. Heyes, D. Dini, and T. A. Zaki, Phys. Rev. E **85**, 056705 (2012).
[21] J.-P. Hansen and I. R. McDonald, *Theory of Simple Liquids*, 3rd ed. (Academic Press, Amsterdam, 2006), p. 32.
[22] P. Schofield and J. R. Henderson, Proc. R. Soc. A (London) **379**, 231 (1982).
[23] N. C. Admal and E. B. Tadmor, J. Elast. **100**, 63 (2010).
[24] C. Hirsch, *Numerical Computation of Internal and External Flows*, 2nd ed. (Elsevier, Amsterdam, 2007).
[25] R. Goetz and R. Lipowsky, J. Chem. Phys. **108**, 7397 (1998).
[26] D. M. Heyes, E. R. Smith, D. Dini, and T. A. Zaki, J. Chem. Phys. **135**, 024512 (2011).
[27] O. H. Ollila, H. J. Risselada, M. Louhivuori, E. Lindahl, I. Vattulainen, and S. J. Marrink, Phys. Rev. Lett. **102**, 078101 (2009).
[28] O. G. Jepps and S. K. Bhatia, Phys. Rev. E **67**, 041206 (2003).
[29] K. S. Cheung and S. Yip, J. Appl. Phys. **70**, 5688 (1991).
[30] N. W. A. van Uden, H. Hubel, D. A. Faux, A. C. Tanczos, B. J. Howlin, and D. J. Dunstan, J. Phys.: Cond. Matt. **15**, 1577 (2003).
[31] W. A. Curtin and E. Miller, Model. Sim. Mater. Sci. Eng. **11**, R33 (2003).
[32] J. Fish, M. A. Nuggehally, M. S. Shephard, C. R. Picu, S. Badia, M. L. Parks, and M. Gubzburger, Comput. Meth. Appl. Mech. Eng. **196**, 4548 (2007).
[33] D. Boda, T. Lukács, J. Liszi, and I. Szalai, Fluid Phase Equilib. **119**, 1 (1996).
[34] G. Michel and D. J. Searles, Phys. Rev. Lett. **110**, 260602 (2013).
[35] N. G. Hadjiconstantinou, A. L. Garcia, M. Z. Bazant, and G. He, J. Comput. Phys. **187**, 274 (2003).
[36] G. De Fabritiis, R. Delgado Buscalioni, and P. Coveney, Phys. Rev. Lett. **97**, 134501 (2006).
[37] H. Stassen and W. A. Steele, J. Chem. Phys. **102**, 932 (1995).
[38] M. Zhou, Proc. R. Soc. A **459**, 2347 (2003).